Aptamer-ligand recognition studied by native ion mobility-mass spectrometry

Aptamer-ligand recognition studied by native ion mobility-mass spectrometry

Elise Daems[a,b], Debbie Dewaele[a], Konstantin Barylyuk[a,1], Karolien De Wael[b], and Frank Sobott[a,c,d,*]

[a] *BAMS Research Group, University of Antwerp, Groenenborgerlaan 171, 2020 Antwerp, Belgium*

[b] *AXES Research Group, University of Antwerp, Groenenborgerlaan 171, 2020 Antwerp, Belgium*

[c] *Astbury Centre for Structural Molecular Biology, University of Leeds, Leeds LS2 9JT, UK*

[d] *School of Molecular and Cellular Biology, University of Leeds, Leeds LS2 9JT, UK*

* E-mail: F.Sobott@leeds.ac.uk

Abstract

The range of applications for aptamers, small oligonucleotide-based receptors binding to their targets with high specificity and affinity, has been steadily expanding. Our understanding of the mechanisms governing aptamer-ligand recognition and binding is however lagging, stymieing the progress in the rational design of new aptamers and optimization of the known ones. Here we demonstrate the capabilities and limitations of native ion mobility-mass spectrometry for the analysis of their higher-order structure and non-covalent interactions. A set of related cocaine-binding aptamers, displaying a range of folding properties and ligand binding affinities, was used as a case study in both positive and negative electrospray ionization modes. Using carefully controlled experimental conditions, we probed their conformational behavior and interactions with the high-affinity ligand quinine as a surrogate for cocaine. The ratios of bound and unbound aptamers in the mass spectra were used to rank them according to their apparent quinine-binding affinity, qualitatively matching the published ranking order. The arrival time differences between the free aptamer and aptamer-quinine complexes were consistent with a small ligand-induced conformational change, and found to inversely correlate with the affinity of binding. This mass spectrometry-based approach provides a fast and convenient way to study the molecular basis of aptamer-ligand recognition.

Keywords: Oligonucleotide structure, Aptamers, Ligand affinity, Native mass spectrometry, Ion Mobility

1. Introduction

Aptamers are oligonucleotide sequences that occur naturally as the sensing part of riboswitches, which are regulatory segments of messenger RNA involved in gene expression [1]. Almost three decades ago, Tuerk *et al.* introduced the Systematic Evolution of Ligand by EXponential enrichment (SELEX) protocol to develop synthetic aptamers as high-affinity binders for target molecules [2]. In essence, aptamers are short single-stranded molecules consisting of approximately 20-80 nucleotides, with a molecular mass of 6-30 kDa. They are characterized by a specific 3D conformation, or fold, which enables high-specificity and high-affinity recognition of the target [3]. Noncovalent interactions such as van-der-Waals forces, hydrogen bonding, electrostatic interactions, and hydrophobic interactions mediate aptamer folding and ligand binding, but the different contributions of these

[1] Present address Konstantin Barylyuk: University of Cambridge, Hopkins Building, Tennis Court Road, Cambridge CB2 1QW, UK.

forces are relatively poorly understood, and molecular modelling approaches are also in their infancy. Nevertheless, aptamers have nowadays been designed to bind small molecules, peptides, proteins, nucleic acids, and even cells [4]. Their high affinity and specificity render them an attractive alternative to monoclonal antibodies, and there is great current interest in their application in diverse fields of biomedicine and analytical science. For example, the use of aptamers as therapeutic agents has several advantages. First, aptamers can have a superior selectivity, specificity and binding affinity to their targets [5]. Second, aptamers are produced in vitro with high reproducibility and purity, which reduces the production costs. Furthermore, aptamer sequences are generally not targeted by the immune system and are therefore not immunogenic [6]. Finally, aptamers are relatively small, chemically stable, and easy to modify [3,7]. Thanks to their unique characteristics and multiple advantages, aptamers has seen a recent resurgence as drug targets and biopharmaceutical agents [8,9], but they are also used for the detection of environmentally important compounds in sensors [7,10].

What is lacking however is a thorough understanding of the relationship between the sequence, and what determines the higher-order structure and specific interactions of aptamers. Currently used techniques to characterize aptamer structure and aptamer-target interactions are mainly nuclear magnetic resonance (NMR) spectroscopy and x-ray crystallography [11,12]. Moreover, biophysical techniques, i.e. isothermal titration calorimetry (ITC) and surface plasmon resonance (SPR), are regularly used to gain more insights into aptamer-target interactions [13,14]. But also mass spectrometry (MS) can provide such tools, which are capable of determining sequence variations and heterogeneity (denatured MS) and link these with 3D structure and interactions (native MS) [15,16]. In recent years, native MS, often in combination with ion mobility (IM) spectrometry, has become an important technique for studies of the structure of biomolecular conformation and interactions [17,18]. The impact of this MS-enabled “structural biology in the gas-phase” is significant; and more recently, the structural characterization and quality control of therapeutic antibodies have also been largely driven by structural MS methods. In contrast, analogous approaches for the structural characterization and quality control of oligonucleotides are recent and not routinely applied in the field. Native MS provides information about the stoichiometry (provided that the affinity is in the low-µmol/L to nmol/L range), and allows simultaneous identification and characterization of individual species in a heterogeneous ensemble [17,18]. This is in contrast to many other structural and biophysical techniques which either require homogeneous sample, or report on the ensemble-average or the most prominent state. Native IM-MS has had a major impact on the study of dynamic and large protein complexes [19,20], but is still largely unexplored for oligonucleotides. It has, however, great potential to connect primary and higher-order structural information of oligonucleotides and their complexes and therefore contribute to the characterization of this molecule class as well.

As an example, Baker *et al.* studied DNA hairpins, pseudoknots, and cruciform structures. The collision cross section (CCS) values measured by IM-MS were compared to those calculated from molecular dynamics simulations and a match was found with the structures of the lowest charge states [21]. More recently, Gabelica and co-workers significantly advanced the application of IM-MS to DNA structure by systematically and comprehensively characterizing G-quadruplexes, their stability, the binding of ligands and the role of counter-ions [22–25]. This has also led to a better understanding of the effect of different instrument tuning parameters on the structure of oligonucleotides and their behavior in the gas-phase [26,27]. In addition, Gülbakan, Barylyuk *et al.* demonstrated that native electrospray ionization (ESI) MS can be used to determine the binding selectivity and stoichiometry of aptamers, but can also provide more information on the binding model [28]. Nevertheless, particularly flexible or disordered protein structures have been found to undergo some degree of gas-phase

"collapse" even under gentle MS conditions, in cases where the free enthalpy barriers for these transitions were low [29]. In contrast to G-quadruplexes which appear rigid, short DNA duplexes were found to compact over 20 % according to their CCS values and compared to canonical B helices [30]. The question therefore arises here how far aptamers retain key characteristics of their structure in the gas-phase, preserving key aspects of their folding and ligand recognition.

In this study, we focus on a set of cocaine-binding aptamers, with a range of binding mechanisms proposed from folding-upon-binding to preformed rigid binders, and their interactions with the ligand quinine [31,32]. Although originally selected to specifically recognize cocaine, cocaine-binding aptamers are known to also bind to other alkaloids and steroids, with up to 30-fold greater affinity toward quinine than cocaine. Reinstein *et al.* proposed that this higher affinity could be explained by the larger bicyclic aromatic ring in the quinine ligand, which probably provides an increase in stacking interactions with the DNA bases of the aptamer [31]. We demonstrate that counter-ions play an important role for stabilization of the higher-order structure of the aptamer, by analyzing aptamer samples prepared in solutions of different ionic strengths. Although the current paradigm postulates that the negative ionization mode is the "natural" one for the analysis of nucleic acids, we show that aptamers and ligand complexes can also be detected and analyzed in the positive mode with high sensitivity and specificity. By comparing the set of aptamers, it becomes apparent that native MS is able to determine relative binding strengths and rank ligands according to their affinity. IM spectrometry allows observation of small conformational changes, which we find to relate to the mode of binding. In summary, we propose native IM-MS as a relatively fast and simple method to study aptamer-ligand interactions, with obvious applications in SELEX panels and aptamer development.

2. Materials and methods

2.1. Materials and sample preparation

All aptamers and the random control sequence derived from MN19 (AAA GTA ACT ACG GAC GGG ATA CCA GCA GTT) were purchased from Eurogentec (Belgium) with a differential precipitation purification method. Ammonium acetate solution (7.5 mol/L, molecular biology grade) and quinine hydrochloride dihydrate (≥ 98.0 %) were purchased from Sigma-Aldrich (Bornem, Belgium). All solutions were prepared using deionized water which had a conductivity of ≤ 0.1 µS/cm after purification using a Silex I B system from Eurowater (Nazareth-Eke, Belgium). All aptamers were dialyzed and buffer-exchanged overnight using Slide-a-Lyzer Mini dialysis units with a molecular weight cut-off of 3.5 kDa (Thermo Fisher Scientific) to 300 mmol/L ammonium acetate pH 6.8 (no pH adjustment required), unless stated otherwise. The buffer was replaced twice during the dialysis. The concentrations of the dialyzed aptamers were verified using a Nanodrop2000 (Thermo Scientific). Extinction coefficients were calculated by the Nanodrop2000 software based on the oligonucleotide sequences. Quinine was solubilized in 300 mmol/L ammonium acetate, after which aptamer-quinine complexes were prepared using a 1:1 aptamer-quinine molar ratio with a final concentration of 5-10 µmol/L and afterwards incubated for a few minutes (no re-annealing was done).

2.2. Native nano-ESI IM-MS

Native nano-ESI-IM-MS analyses were performed on a Synapt G2 HDMS Q-TOF instrument (Waters, Manchester, UK). Approximately 3-5 µl of sample was introduced into the mass spectrometer, using nano-ESI with gold-coated borosilicate glass tapered-tip capillaries made in-house. Experiments were performed in both the positive and the negative ionization mode. The instrument was carefully tuned to balance preservation of native structure with achieving sufficient declustering, in order to obtain

well-resolved spectra. Figure S-1 shows the effect of tuning three key parameters which control ion activation (internal energy) on the survival of aptamer-ligand complexes. The voltages employed here are shown to retain ca. 50 % of the noncovalent complex present. The following settings were used: spray capillary voltage 1.0-1.4 kV, source temperature 30 °C, sampling cone 25 V in positive and 20 V in negative ionization mode, extraction cone 1 V in positive and 5 V in negative ionization mode, trap collision energy 5 V, transfer collision energy 0 V, trap DC bias 45 V, IMS wave height 35 V and IMS wave velocity 800 m/s. The backing pressure was set to 2.75 mbar, the source pressure to $2.34 \cdot 10^{-3}$ mbar in the positive ionization mode and $1.51 \cdot 10^{-3}$ mbar in the negative ionization mode, the trap pressure to $2.38 \cdot 10^{-2}$ mbar, the IMS pressure to 2.98 mbar, the transfer pressure to $2.50 \cdot 10^{-2}$ mbar. An overview of these settings is provided in Table S-1. All data were analyzed using MassLynx 4.1 and Driftscope (Waters). The relative abundances of all species were calculated by integrating the peak areas of each species. Arrival time profiles were extracted using the full width at half maximum (FWHM) of the peaks without adducts. An overview of all m/z-values used for extraction of the arrival times is shown in Table S-2.

3. Results and discussion

In this study, we use a set of closely related DNA-based cocaine-binding aptamers as model compounds for the comparative native MS analysis. Four cocaine-binding aptamers were chosen: MN19, MNS-7.9, MN4 and 38-GC (Figure 1). Their structure contains three stems built around a three-way junction, which is the proposed binding pocket [33]. The second stem contains only Watson-Crick base pairs, whereas stems 1 and 3 contain non-canonical base pairs. When aligned, the sequences only differ in their terminal parts and at position 24 of the consensus sequence (Figure S-2). The MNS-7.9 and MN19 aptamers consist of 30 nucleotide residues, with the only difference being the base pair at position 24 (compared to the consensus), where the C has been replaced with T. The MN19 aptamer has a dissociation constant K_d of 26.7 µmol/L for cocaine (obtained in 20 mmol/L Tris (pH 7.4), 140 mmol/L NaCl, and 5 mmol/L KCl) and is reported as a loosely folded structure [31]. The MNS-7.9 aptamer has a corresponding K_d of 20 µmol/L (obtained in the same buffer as the K_d of MN19) and is described as structurally very flexible [33]. Roncancio *et al.* developed the 38-GC sequence (38 bases) by modifying the existing aptamer MNS-4.1, resulting in a higher affinity for cocaine binding (K_d value for cocaine: 2.6 µmol/L obtained in 10 mmol/L Tris buffer (pH 7.4) with 0.01 mmol/L $MgCl_2$ and 5% DMSO). They stabilized the 38-GC aptamer by (i) replacing the non-canonical base pairs in MNS-4.1 with Watson-Crick base pairs and (ii) by converting the G-T wobble pair in the stem 3 to a matched G-C base pair. As a result, the 38-GC aptamer is characterized by a rigid structure, which stably folds in the absence of ligand at room temperature [34]. The fourth aptamer MN4 consists of 36 bases, has a K_d value of 7 µmol/L for cocaine (obtained in the same buffer as the K_d of MN19 and MNS-7.9) and is described in the literature as structurally rigid [31,35,36]. Although all these aptamers were originally selected to specifically recognize cocaine, they bind quinine with a higher affinity [31]. Therefore, quinine was chosen as ligand in this study as a surrogate for cocaine.

3.1. Ionic strength in solution is crucial for preservation of the aptamer fold in the negative ionization mode

The presence of cations is an important factor for the structure and stability of oligonucleotides in general; they act as counter-ions to the negatively charged phosphate backbone. For example, high concentrations of monovalent cations (i.e. Na^+ and K^+) stabilize DNA duplexes, resulting in higher melting temperatures [37]. Divalent Mg^{2+}-ions are even more important *in vivo*, because not only do

they stabilize the structure but also facilitate the folding of duplexes into secondary and tertiary structures [38]. Such effects are also expected for aptamers [39], and here we studied the effect of the ionic strength of the solution on the structure of aptamers. We tested several concentrations of ammonium acetate, which is commonly used in native IM-MS, (50 to 300 mmol/L in water, pH 6.8) as well as pure water to probe the effect of the ionic strength on the charge state distribution of the MN19 aptamer in both negative and positive ionization mode. In native MS of proteins, the amount of charging observed due to multiple (de-)protonation events correlates well with the extent of the exposed surface area, which in turn depends on the compactness of the structure [40].

In the negative ionization mode, the charge states we observed ranged from 18- to 7- in water (Figure S-3A). Increasing the ionic strength to 50 mmol/L ammonium acetate resulted in a shift to lower values (12- to 5-), and from 100 mmol/L onwards only 6-, 5-, and 4- ions were observed. These observations highlight that the presence of ions, here ammonium and acetate, plays an important role for the charge state distribution of single-stranded DNA aptamers (Figure 2A). The presence of highly charged species, represented by the 14- charge state, would indicate an extended form of the aptamer in the absence of counter-ions. In 50 mmol/L ammonium acetate, this extended state disappears while an intermediate state, represented by the 6- charge state, shows up together with the compact state centered on the 5- charge state. From 100 mmol/L onwards, this narrow distribution around 5- persists, implying compact structures of the aptamers [41]. In the positive ionization mode, only the 5+ and 4+ charge states of aptamer ions, representing compact structures, were present in the spectra throughout the whole range of ionic strengths (Figure S-3B). In contrast to the negative ionization mode, no highly charged species were present at low ionic strength (Figure 2B). This has also been previously observed for i-motifs [42].

The interesting observation, that the aptamer only appears highly charged without buffer in the negative ionization mode, is explained by the lack of counter-ions, which would otherwise reduce the net charge in the highly acidic phosphate backbone. Coulombic repulsion destabilizes the structure in solution, as is well known for DNA [43], but would also prevent refolding or compaction of the desolvated and highly charged i.e. extended ions in the gas-phase [30]. This is further supported by the findings of Sharawy *et al.*, who performed molecular dynamics simulations of negatively charged electrospray nanodroplets containing a double-stranded DNA [44]. In the positive ionization mode, protonation during ESI diminishes this charge density in the backbone so that the oligonucleotides are more likely to be released as compact molecules. At the same time, high positive charge states cannot be reached without sufficient ammonium ions present which can protonate the oligonucleotide (via adduct formation, with volatile ammonia lost during ESI).

When using ion mobility, the arrival time (or derived CCS) can provide detailed insights into the structure of an aptamer in the gas-phase [41]. We compared the arrival times for the 5- and 5+ “compact” charge state over the range of ionic strengths (Figure 2C). The error of all arrival times is limited by the time resolution of the measurement and can be estimated as ± 0.055 ms. Assuming this level of accuracy, we observed only minor deviation in the measured arrival times of the 5- and 5+ aptamer ions electrosprayed from solutions with different ionic strengths, suggesting that there were no major structural differences for this particular charge state. A consistent, albeit small difference is seen between the negative and the positive ionization mode, with the positive form appearing slightly more compact (lower arrival times). The same is true for the 4- and 4+ charge state (Figure S-4). These small differences may be linked to asymmetries in the instrument settings for negative and positive ions, and can also be caused by slightly different long-range interactions of the analyte ions with the drift gas, but their origin cannot be conclusively determined within the scope of the present work. Importantly, while the appearance and extent of the charge state distributions was found to depend

on the ionic strength and ionization mode used, no significant differences were observed in the arrival time of a specific charge state.

The MS and IM data in this study are in agreement with previous observations in literature where the use of ≥ 100 mmol/L ammonium acetate was considered to be a "native" buffer for ESI MS [30]. But more importantly, this also corroborates the fact that cations are of great significance for the structure and stability of DNA, including aptamers [37,38,45].

3.2. Native IM-MS detects MN19-quinine complexes and indicates a conformational change upon ligand binding

In order to investigate ligand binding to the cocaine-binding aptamers, quinine was chosen because of its higher affinity than cocaine (see above), meaning that quinine concentrations are more amenable to the native MS analysis . The dissociation constant K_d of MN19 aptamer complexes was previously determined to be 0.7 ± 0.2 µmol/L for quinine and 26.7 ± 0.7 µmol/L for cocaine using ITC [31]. These values are averages of 2-5 individual ITC experiments and the reported error is the standard deviation.

A 300 mmol/L ammonium acetate solution was selected here for the IM-MS experiments, since an ionic strength of at least 100 mmol/L was found to be necessary to preserve the folded structure (see above), and fewer non-volatile adducts are present at higher buffer concentration. The addition of quinine to MN19 at 1:1 molar ratio resulted in the formation of ligand-aptamer complexes that were detected in both negative and positive ionization mode, albeit at different relative signal intensities (Figure 3). In the negative ionization mode, 41 % of the aptamer is complexed, while in the positive mode only 18 % of the aptamer binds to quinine. These results demonstrate an effect of the ionization mode on the preservation of non-covalent complexes of oligonucleotides and ligands upon transfer from the solution to the gas-phase. A higher amount of a ligand bound to DNA in the negative ionization mode than in the positive ionization mode was also observed before by Rosu *et al.* [46]. We attribute the observed difference in the relative intensity of the complex signal to the charge localization in both ionization modes. In the negative mode, the charges are localized mostly on the phosphate groups of the sugar phosphodiester backbone, whereas positive charges are expected on the nucleobases with the phosphate backbone largely neutralized [47]. The ligand itself can also become charged; the pKa values of the quinuclidinyl and quinolone group of quinine at 20 °C are 4.1 and 8.5, respectively. Hence, quinine is positively charged at neutral pH in solution [48], causing repulsion with the positive charges near the nucleobase interaction site and weakening the interaction in the positive, but not in the negative ionization mode.

In general, the amount of complex detected was lower than expected, given the K_d values in the nmol/L range previously reported. For example, over 88 % of MN19 (K_d = 0.7 µmol/L) is expected to bind quinine at a concentration of both aptamer and ligand equal to 5 µmol/L, whereas only up to 41 % (or 18 % in the positive ionization mode) of the aptamer showed complexation in our experiments. A likely explanation for this difference lies in the instrument tuning parameters which were chosen here to achieve good peak resolution. Particularly the used Trap DC bias voltage has a slight activating effect, accounting for roughly 50 % ligand loss (see Figure S-1). A possible additional effect is due to the contribution of hydrophobic interactions to ligand binding. Hydrophobic interactions are known to be absent in the gas-phase (as they rely on the tendency of water to sequester nonpolar solutes), thereby shifting the balance of attractive forces which keep ligands bound, and potentially leading to a weakening of the complex upon transfer from solution to the gas-phase [49,50]. This is in contrast to electrostatic interactions which are strengthened in the absence of water in the gas-phase. The observation that we can detect ligand binding, but not in a quantitative manner, indicates that the

binding is not purely charge-driven [51]. Finally, also the exact buffer and concentration (here 300 mmol/L ammonium acetate), as well as the temperature (in our case room temperature), can influence the affinity of the aptamer compared to other methods.

In order to investigate the effect of ligand binding on the structure of an aptamer, we used ion mobility again. The extracted arrival times of the 5- and 5+ charge state of the MN19 aptamer and the corresponding aptamer-quinine complex are shown in Figure S-5. Upon addition of quinine, shifts towards higher arrival times of 5.0 % and 6.4 % respectively in the negative and positive ionization modes are observed. Based on the arrival time resolution alone, an error of 0.055 ms or 0.25% is expected but accuracies of ≤ 2% are commonly accepted for this instrumental setup [52]. This means that the detected differences are similar in both polarities, and significant: the binding of the ligand has an observable effect on the structure of the aptamer in the gas-phase. The additional size of the ligand alone, if it were to bind peripherally (i.e. add to the overall volume), compared to the size of the aptamer would not explain the observed difference in arrival time. For the MN19 aptamer there is a 3.4% mass increase upon binding to quinine; assuming a proportional volume increase, an estimate can be made that the additional molecular volume would only correspond to a 2.3% increase in arrival time (which correlates with the cross section, i.e. scales with volume$^{2/3}$; and less if the ligand were to bind inside a pocket). This is significantly less than the observed 6.4% (or 5.0 %) increase, which we therefore expect to be caused by a conformational change of the aptamer upon binding.

Two extreme cases for binding mechanisms can be considered: folding-upon-binding and binding to preformed aptamers (conformational selection) (Figure 4). Folding-upon-binding would correspond to a significant conformational change of the global 3D structure upon binding of the ligand, but no corresponding shift in the charge state distribution of the aptamer peaks is seen (data not shown). The observed, relatively small change in arrival time does also not support this model. Binding of the ligand to a preformed, completely rigid aptamer on the other hand is also rather unlikely, since this would not result in an observable arrival time increase beyond the small amount due to the volume of the ligand itself. The observation of a significant, but relatively small change in arrival time suggests that the aptamer broadly retained its fold and only more subtle conformational changes occurred. Interestingly also to observe that the arrival time was found to increase upon ligand binding.

These findings can be interpreted in the context of the literature. For the MN19 aptamer with 3 base pairs in stem 1, the three-way junction was proposed as the binding site [31,33]. Moreover, Cekan *et al.* suggested a binding model based on EPR and fluorescence data, where stem 2 and 3 are already folded without a ligand while stem 1 is not formed and only folds upon binding of the ligand [53]. This model was later confirmed by Neves *et al.* for the MN19 aptamer specifically using NMR spectroscopy [54]. These findings are reflected in our IM-MS data of the aptamer and complex, which corroborate that the aptamer-ligand complex formation occurs with a small conformational change. Specifically it seems that binding is accompanied by a slight extension of the structure, as evidenced by the increase in arrival time.

3.3. Native IM-MS captures trends in ligand affinity and conformational dynamics of increasingly more rigid cocaine-binding aptamers

The IM-MS approach was extended in the positive ionization mode to a panel of cocaine-binding aptamers (MN19, MNS-7.9, MN4 and 38-GC) to test the ability of the method to differentiate between closely related aptamer structures, and how their relative ligand binding affinities differ. These aptamers exhibit a range of binding properties; it was previously shown that mainly stem 1 determines the binding behavior [32]. For example, the MN4 aptamer, which has a long stem 1 (6 base pairs), has

been described with a well-defined structure in its free and bound forms. By contrast, the MN19 aptamer, which has a shortened stem 1 (3 base pairs), has a rather loose and unstructured conformation and only becomes structured after ligand binding [31,32].

A randomized sequence, with the same composition as the MN19 aptamer, was used as a control. Upon adding quinine (1:1 ratio) to this sequence, no complex was formed proving that there is no non-specific binding under the conditions used (Figure 5A and Figure S-6). The addition of quinine to the cocaine-binding sequences resulted in ligand-aptamer complexes. Importantly, the amount of complex formed differed for all cocaine-binding aptamers, reflecting their differences in binding affinity, albeit not in a quantitative fashion (see discussion above for MN19). The affinity to quinine has been determined previously by ITC only for some of the aptamers studied here (see Table S-3). Nevertheless, it was shown before by comparing multiple aptamers that the relative affinity towards cocaine is a measure for the relative affinity towards quinine and vice versa [31,54]. In native IM-MS, the relative complex signal intensity upon adding quinine at a 1:1 molar ratio varies systematically between the different aptamers (Figure 5). The MN19 aptamer, which has the highest K_d value among them, binds the least quinine (22%). On the other hand, the aptamer with the lowest K_d (38-GC) binds the most quinine (43%). In general, there is a clear trend in the signal intensity of the complex in agreement with the expected trend in the solution-phase binding affinity. These results show that native ESI-MS can be used to determine relative, albeit not absolute binding strengths of aptamers correctly, based on the intensity ratio of complex and aptamer signals, confirming previously reported data in the literature [31,33,34,54].

In a next step, we investigated the influence of ligand binding on aptamer structure. Upon addition of quinine, arrival time increases ranging from 3.9% to 6.4% were observed for the different aptamers (Figure 5B). As for the MN19 aptamer, these changes in arrival time cannot be assigned to the additional size of the ligand compared to the size of the aptamers alone, which would only account for a maximum of 2.0 - 2.3 % increase in arrival time for peripheral binding (and less for occluded binding). The same interpretation of the arrival time shifts can be followed for all aptamers: The relatively small increase in arrival time upon binding, and the observation that no charge state shifts occur, suggests that complex formation did not result in a dramatic conformational change of the global 3D structure (which folding-upon-binding would cause). The aptamers seemed to broadly retain their fold and only more subtle conformational changes occurred, which are most likely due to the behavior of stem 1. There are some interesting differences however between the aptamers (Figure 5B). With increasing length of stem 1 from MN19 to MN4 and 38-GC, the arrival time differences upon complexation showed a downward trend from 6.4 % to 4.2 % and 3.9 %, respectively, while at the same time binding affinity increased (lower K_d). We propose that the more preformed, “rigid” binding e.g. seen in MN4 leads to less structural rearrangement upon complexation (as evidenced by the smaller arrival time changes) accompanied by a higher binding affinity (Figure 5A), whereas the more adaptive binding suggested for MN19 requires more reorganization and comes with a lower ligand affinity, possibly due to an entropic penalty [31]. The key difference between these aptamers is the length of stem 1, but without detailed structural models we can only speculate why ligand binding leads to a slight size increase of the overall structure. The results obtained with IM-MS are broadly consistent with data in literature obtained with NMR and small-angle X-ray scattering (SAXS) by Reinstein *et al.* and Neves *et al.* [31,32].

4. Conclusion

We reported here the use of native IM-MS to analyze cocaine-binding aptamers in the negative and positive ionization mode; specifically, their higher-order structure and non-covalent interactions. The

data showed that counter-ions play an important role in stabilizing the folded form of the aptamers in the negative ionization mode upon transfer from the solution to the gas-phase. This is due to the negatively charged phosphate backbone which leads to significant intramolecular charge repulsion, both in solution and in the gas-phase, and reflects the key role cations are known to have in stabilizing oligonucleotide higher-order structure in solution. Positive charges on the other hand are due to protonation during ESI and differently distributed throughout the molecule, and only low-charged compact states are detected in the spectra. The use of buffers with an ionic strength of 100 mmol/L ammonium acetate or higher was previously reported as "native" solution conditions in native MS.

Moreover, it was demonstrated that aptamer-ligand complexes can be detected and analyzed in the positive ionization mode native IM-MS, despite the previously claimed superiority of the negative ionization mode for the analysis of nucleic acids. Advantages of being able to work in the positive ionization mode are for example that ion mobility calibrants are more readily available, and that protein-oligonucleotide complexes are usually studied in the same ionization mode. Native MS can also determine relative binding affinities of a set of cocaine-binding aptamers by using the ratio of the bound and unbound peak in the mass spectra; the ranking order thus obtained matches known complex stabilities (K_d values). The approach has proven to be sensitive towards small structural alterations of the aptamer, and since a randomized sequence did not show any binding, we conclude that there are only selective interactions occurring under the conditions used in this study. The fact that less complex was observed as expected from the reported solution-phase binding affinity is largely explained by the chosen instrument tuning settings.

Ion mobility data gave insight into structural differences between the aptamers upon ligand binding. Each charge state appeared to have a defined arrival time irrespective of ionization polarity and ionic strength of the solution (although certain charge states were absent without sufficient counter-ions), within the error margin of the overall experiment (≤ 2 %). Ion mobility experiments allowed determination of subtle conformational changes within one charge state, when comparing the structure of different aptamers and also detecting structural effects of ligand binding. The magnitude of the change was found to correlate with the binding mode, with the more pre-formed and rigid aptamers such as the long-stem MN4 showing higher binding affinity but a smaller arrival time increase. It is important to note though that double stranded DNA is expected to undergo compaction during transfer from the solution to the gas-phase [30,44], and this can reasonably be expected to also occur in aptamers. We did therefore not attempt to determine the actual CCS values, although this will be of great interest in a future study, but carefully observed arrival time shifts, i.e. relative differences, under identical experimental conditions. These shifts gave nevertheless an insightful qualitative, arguably semi-quantitative, picture of structural differences between aptamers and upon ligand binding, allowing us to infer tenets of the binding mechanism and the structural reorganization which accompanies ligand recognition.

We showed that native MS combined with IM can contribute to the understanding of the higher-order structure of aptamers and their complexes. Although this structural MS method stands strong in itself, combining it with other structural and computational approaches holds considerable promise towards a deeper understanding of oligonucleotide higher-order structure and function. This perspective will be worthwhile exploring in future oligonucleotide-oriented research.

Acknowledgements

Funding: This work was supported by the Fund for Scientific Research (FWO) Flanders [grant number 1S65717N].

Appendix: Supplementary material

References

[1] N.G. Walter, D.R. Engelke, Ribozymes: Catalytic RNAs that cut things, make things, and do odd and useful jobs, Biol. 49 (2002) 199–203.

[2] C. Tuerk, L. Gold, Systematic evolution of ligands by exponential enrichment: RNA ligands to bacteriophage T4 DNA polymerase, Science. 249 (1990) 505–510. https://doi.org/10.1126/science.2200121.

[3] H. Sun, Y. Zu, A highlight of recent advances in aptamer technology and its application, Molecules. 20 (2015) 11959–11980. https://doi.org/10.3390/molecules200711959.

[4] A. Chen, S. Yang, Replacing antibodies with aptamers in lateral flow immunoassay, Biosens. Bioelectron. 71 (2015) 230–242. https://doi.org/10.1016/j.bios.2015.04.041.

[5] K. Gebhardt, A. Shokraei, E. Babaie, B.H. Lindqvist, RNA aptamers to S-adenosylhomocysteine: Kinetic properties, divalent cation dependency, and comparison with anti-S-adenosylhomocysteine antibody, Biochemistry. 39 (2000) 7255–7265. https://doi.org/10.1021/bi000295t.

[6] A.D. Keefe, S. Pai, A. Ellington, Aptamers as therapeutics, Nat. Rev. Drug Discov. 9 (2010) 537–550. https://doi.org/10.1038/nrd3141.

[7] S. Song, L. Wang, J. Li, J. Zhao, C. Fan, Aptamer-based biosensors, Trends Anal. Chem. 27 (2008) 108–117. https://doi.org/10.1016/j.trac.2007.12.004.

[8] Y. Chen, T. Hong, S. Wang, J. Mo, T. Tian, X. Zhou, Epigenetic modification of nucleic acids: From basic studies to medical applications, Chem. Soc. Rev. 46 (2017) 2844–2872. https://doi.org/10.1039/c6cs00599c.

[9] S.M. Nimjee, R.R. White, R.C. Becker, B.A. Sullenger, Aptamers as therapeutics, Annu. Rev. Pharmacol. Toxicol. 57 (2017) 61–79. https://doi.org/10.1146/annurev-pharmtox-010716-104558.

[10] M. Ilgu, M. Nilsen-Hamilton, Aptamers in analytics, Analyst. 141 (2016) 1551–1558. https://doi.org/10.1039/c5an01824b.

[11] T. Sakamoto, NMR study of aptamers, Aptamers. 1 (2017) 13–18.

[12] A.A. Novoseltseva, E.G. Zavyalova, A. V Golovin, A.M. Kopylov, An insight into aptamer-protein complexes, Aptamers. 2 (2018) 55–63.

[13] T. Sakamoto, E. Ennifar, Y. Nakamura, Thermodynamic study of aptamers binding to their target proteins, Biochimie. 145 (2018) 91–97. https://doi.org/10.1016/j.biochi.2017.10.010.

[14] E. González-Fernández, N. De-Los-Santos-Álvarez, A.J. Miranda-Ordieres, M.J. Lobo-Castañón, SPR evaluation of binding kinetics and affinity study of modified RNA aptamers towards small molecules, Talanta. 99 (2012) 767–773. https://doi.org/10.1016/j.talanta.2012.07.019.

[15] A.C. Leney, A.J.R. Heck, Native mass spectrometry: What is in the name?, J. Am. Soc. Mass Spectrom. 28 (2017) 5–13. https://doi.org/10.1007/s13361-016-1545-3.

[16] S. Schürch, Characterization of nucleic acids by tandem mass spectrometry - the second decade (2004-2013): From DNA to RNA and modified sequences, Mass Spectrom. Rev. 35 (2016) 483–523. https://doi.org/10.1002/mas.

[17] E. Boeri Erba, C. Petosa, The emerging role of native mass spectrometry in characterizing the structure and dynamics of macromolecular complexes, Protein Sci. 24 (2015) 1176–1192. https://doi.org/10.1002/pro.2661.

[18] F. Sobott, M.G. Mccammon, H. Hernández, C. V. Robinson, The flight of macromolecular complexes in a mass spectrometer, Philos. Trans. R. Soc. A Math. Phys. Eng. Sci. 363 (2005) 379–391. https://doi.org/10.1098/rsta.2004.1498.

[19] C. Uetrecht, R.J. Rose, E. Van Duijn, K. Lorenzen, A.J.R. Heck, Ion mobility mass spectrometry of proteins and protein assemblies, Chem. Soc. Rev. 39 (2010) 1633–1655. https://doi.org/10.1039/b914002f.

[20] F. Lanucara, S.W. Holman, C.J. Gray, C.E. Eyers, The power of ion mobility-mass spectrometry for structural characterization and the study of conformational dynamics, Nat. Chem. 6 (2014) 281–294. https://doi.org/10.1038/nchem.1889.

[21] E.S. Baker, N.F. Dupuis, M.T. Bowers, DNA hairpin, pseudoknot, and cruciform stability in a solvent-free environment, J. Phys. Chem. B. 113 (2009) 1722–1727. https://doi.org/10.1021/jp807529m.

[22] A. Marchand, V. Gabelica, Native electrospray mass spectrometry of DNA G-quadruplexes in potassium solution, J. Am. Soc. Mass Spectrom. 25 (2014) 1146–1154. https://doi.org/10.1007/s13361-014-0890-3.

[23] R. Ferreira, A. Marchand, V. Gabelica, Mass spectrometry and ion mobility spectrometry of G-quadruplexes. A study of solvent effects on dimer formation and structural transitions in the telomeric DNA sequence d(TAGGGTTAGGGT), Methods. 57 (2012) 56–63. https://doi.org/10.1016/j.ymeth.2012.03.021.

[24] A. Marchand, F. Rosu, R. Zenobi, V. Gabelica, Thermal denaturation of DNA G-quadruplexes and their complexes with ligands: Thermodynamic analysis of the multiple states revealed by mass spectrometry, J. Am. Chem. Soc. 140 (2018) 12553–12565. https://doi.org/10.1021/jacs.8b07302.

[25] V. Gabelica, E.S. Baker, M.P. Teulade-Fichou, E. De Pauw, M.T. Bowers, Stabilization and structure of telomeric and c-myc region intramolecular G-quadruplexes: The role of central cations and small planar ligands, J. Am. Chem. Soc. 129 (2007) 895–904. https://doi.org/10.1021/ja065989p.

[26] F. Balthasart, J. Plavec, V. Gabelica, Ammonium ion binding to DNA G-quadruplexes: Do electrospray mass spectra faithfully reflect the solution-phase species?, J. Am. Soc. Mass Spectrom. 24 (2013) 1–8. https://doi.org/10.1007/s13361-012-0499-3.

[27] V. Gabelica, S. Livet, F. Rosu, Optimizing native ion mobility Q-TOF in helium and nitrogen for very fragile noncovalent structures, J. Am. Soc. Mass Spectrom. 29 (2018) 2189–2198. https://doi.org/10.1007/s13361-018-2029-4.

[28] B. Gülbakan, K. Barylyuk, P. Schneider, M. Pillong, G. Schneider, R. Zenobi, Native electrospray ionization mass spectrometry reveals multiple facets of aptamer-ligand interactions: From mechanism to binding constants, J. Am. Chem. Soc. 140 (2018) 7486–7497. https://doi.org/10.1021/jacs.7b13044.

[29] S. Vahidi, B.B. Stocks, L. Konermann, Partially Disordered Proteins Studied by Ion Mobility-Mass Spectrometry: Implications for the Preservation of Solution Phase Structure in the Gas Phase, Anal. Chem. 85 (2013) 10471–10478. https://doi.org/10.1021/ac402490r.

[30] M. Porrini, F. Rosu, C. Rabin, L. Darré, H. Gómez, M. Orozco, V. Gabelica, Compaction of duplex nucleic acids upon native electrospray mass spectrometry, ACS Cent. Sci. 3 (2017) 454–461. https://doi.org/10.1021/acscentsci.7b00084.

[31] O. Reinstein, M. Yoo, C. Han, T. Palmo, S.A. Beckham, M.C.J. Wilce, P.E. Johnson, Quinine binding by the cocaine-binding aptamer. Thermodynamic and hydrodynamic analysis of high-affinity binding of an off-target ligand, Biochemistry. 52 (2013) 8652–8662. https://doi.org/10.1021/bi4010039.

[32] M.A.D. Neves, O. Reinstein, P.E. Johnson, Defining a stem length-dependent binding mechanism for the cocaine-binding aptamer. A combined NMR and calorimetry study., Biochemistry. 49 (2010) 8478–87. https://doi.org/10.1021/bi100952k.

[33] M.N. Stojanovic, P. De Prada, D.W. Landry, Aptamer-based folding fluorescent sensor for cocaine, J. Am. Chem. Soc. 123 (2001) 4928–4931. https://doi.org/10.1021/ja0038171.

[34] D. Roncancio, H. Yu, X. Xu, S. Wu, R. Liu, J. Debord, X. Lou, Y. Xiao, A label-free aptamer-fluorophore assembly for rapid and specific detection of cocaine in biofluids, Anal. Chem. 86 (2014) 11100–11106. https://doi.org/10.1021/ac503360n.

[35] M.A.D. Neves, C. Blaszykowski, S. Bokhari, M. Thompson, Ultra-high frequency piezoelectric aptasensor for the label-free detection of cocaine, Biosens. Bioelectron. 72 (2015) 383–392. https://doi.org/10.1016/j.bios.2015.05.038.

[36] J.E. Smith, D.K. Griffin, J.K. Leny, J.A. Hagen, J.L. Chávez, N. Kelley-Loughnane, Colorimetric detection with aptamer-gold nanoparticle conjugates coupled to an android-based color analysis application for use in the field, Talanta. 121 (2014) 247–255. https://doi.org/10.1016/j.talanta.2013.12.062.

[37] J. Marmur, P. Doty, Determination of the base composition of deoxyribonucleic acid from its thermal denaturation temperature, J. Mol. Biol. 5 (1962) 109–118. https://doi.org/10.1016/S0022-2836(62)80066-7.

[38] D.E. Draper, V.K. Misra, On the role of magnesium ions in RNA stability, Biopolymers. 48 (1998) 113–135. https://doi.org/10.1002/(SICI)1097-0282(1998)48:2<113::AID-BIP3>3.0.CO;2-Y.

[39] J. Lipfert, S. Doniach, R. Das, D. Herschlag, Understanding nucleic acid–ion interactions, Annu. Rev. Biochem. 83 (2014) 813-841. https://doi.org/10.1146/annurev-biochem-060409-092720.

[40] L. Testa, S. Brocca, R. Grandori, Charge-surface correlation in electrospray ionization of folded and unfolded proteins, Anal. Chem. 83 (2011) 6459–6463. https://doi.org/10.1021/ac201740z.

[41] R. Beveridge, S. Covill, K.J. Pacholarz, J.M.D. Kalapothakis, C.E. MacPhee, P.E. Barran, A mass-spectrometry-based framework to define the extent of disorder in proteins, Anal. Chem. 86 (2014) 10979–10991. https://doi.org/10.1021/ac5027435.

[42] A. Garabedian, D. Butcher, J.L. Lippens, J. Miksovska, P.P. Chapagain, D. Fabris, M.E. Ridgeway, M.A. Park, F. Fernandez-Lima, Structures of the kinetically trapped i-motif DNA intermediates, Phys. Chem. Chem. Phys. 18 (2016) 26691–26702. https://doi.org/10.1039/c6cp04418b.

[43] P. Várnai, K. Zakrzewska, DNA and its counterions: A molecular dynamics study, Nucleic Acids Res. 32 (2004) 4269–4280. https://doi.org/10.1093/nar/gkh765.

[44] M. Sharawy, S. Consta, How do non-covalent complexes dissociate in droplets? A case study of the desolvation of dsDNA from a charged aqueous nanodrop, Phys. Chem. Chem. Phys. 17 (2015) 25550–25562. https://doi.org/10.1039/c5cp04331j.

[45] R. Owczarzy, B.G. Moreira, Y. You, M.A. Behlke, J.A. Wälder, Predicting stability of DNA duplexes in solutions containing magnesium and monovalent cations, Biochemistry. 47 (2008) 5336–5353. https://doi.org/10.1021/bi702363u.

[46] F. Rosu, S. Pirotte, E. De Pauw, V. Gabelica, Positive and negative ion mode ESI-MS and MS/MS for studying drug-DNA complexes, Int. J. Mass Spectrom. 253 (2006) 156–171. https://doi.org/10.1016/j.ijms.2005.11.027.

[47] K.A. Sannes-Lowery, D.P. Mack, P. Hu, H.Y. Mei, J.A. Loo, Positive ion electrospray ionization mass spectrometry of oligonucleotides, J. Am. Soc. Mass Spectrom. 8 (1997) 90–95. https://doi.org/10.1016/S1044-0305(96)00202-4.

[48] S. Strauch, J.B. Dressmann, V.P. Shah, S. Kopp, J.E. Polli, D.M. Barends, Biowaiver monographs for immediate-release solid oral dosage forms: Quinine sulfate, J. Pharm. Sci. 101 (2012) 499–508. https://doi.org/10.1002/jps.22810.

[49] M. Sharon, C. V. Robinson, A quantitative perspective on hydrophobic interactions in the gas-phase, Curr. Proteomics. 8 (2011) 47–58. https://doi.org/10.2174/157016411794697363.

[50] C. V Robinson, E.W. Chung, B.B. Kragelund, J. Knudsen, R.T. Aplin, F.M. Poulsen, C.M. Dobson, Probing the nature of non-covalent protein ligand interactions by mass spectrometry, J. Am. Chem. Soc. 118 (1996) 8646–8653. https://doi.org/10.1016/0005-2760(87)90130-5.

[51] J.A. Loo, Electrospray ionization mass spectrometry: A technology for studying noncovalent macromolecular complexes, Int. J. Mass Spectrom. 200 (2000) 175–186. https://doi.org/10.1016/S1387-3806(00)00298-0.

[52] V. Gabelica, A.A. Shvartsburg, C. Afonso, P. Barran, J.L.P. Benesch, C. Bleiholder, M.T. Bowers, A. Bilbao, M.F. Bush, J.L. Campbell, I.D.G. Campuzano, T. Causon, B.H. Clowers, C.S. Creaser, E. De Pauw, J. Far, F. Fernandez-Lima, J.C. Fjeldsted, K. Giles, M. Groessl, C.J. Hogan, S. Hann, H.I. Kim, R.T. Kurulugama, J.C. May, J.A. McLean, K. Pagel, K. Richardson, M.E. Ridgeway, F. Rosu, F. Sobott, K. Thalassinos, S.J. Valentine, T. Wyttenbach, Recommendations for reporting ion mobility mass spectrometry measurements, Mass Spectrom. Rev. 38 (2019) 291–320. https://doi.org/10.1002/mas.21585.

[53] P. Cekan, E.Ö. Jonsson, S.T. Sigurdsson, Folding of the cocaine aptamer studied by EPR and fluorescence spectroscopies using the bifunctional spectroscopic probe Ç, Nucleic Acids Res. 37 (2009) 3990–3995. https://doi.org/10.1093/nar/gkp277.

[54] M.A.D. Neves, A.A. Shoara, O. Reinstein, O. Abbasi Borhani, T.R. Martin, P.E. Johnson, Optimizing stem length to improve ligand selectivity in a structure-switching cocaine-binding aptamer, ACS Sensors. 2 (2017) 1539–1545. https://doi.org/10.1021/acssensors.7b00619.

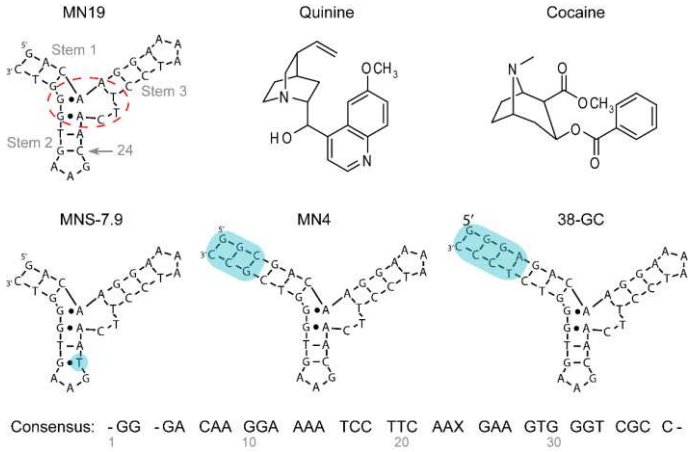

Figure 1. Secondary structures of the cocaine-binding aptamers used in this study, the consensus sequence where X stands for C or T (bottom), and chemical structures of the quinine and cocaine ligands (top right). Watson-Crick base pairs are indicated with dashes and non-Watson-Crick base pairs are shown as dots. The ligand binding site is indicated with a red dashed ellipse. Differences in aptamer sequence compared to the MN19 aptamer are indicated with a blue background.

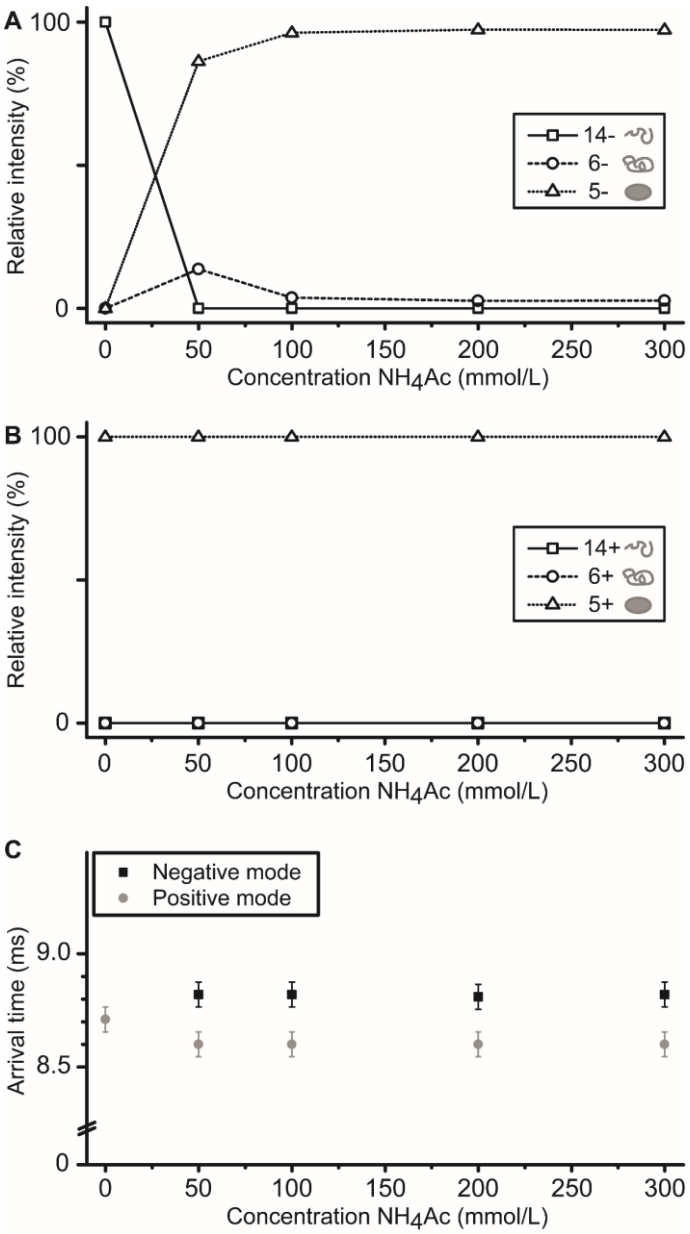

Figure 2. Native MS of the MN19 cocaine-binding aptamer in water, 50, 100, 200, and 300 mmol/L ammonium acetate (NH_4Ac) in (A) the negative and (B) the positive ionization mode. The relative intensity of the three distributions (extended, intermediate and compact state which are represented by the 14, 6 and 5 charge state) is shown (see Figure S-3 for corresponding spectra). (C) Extracted arrival times of the 5-/5+ charge state of the MN19 cocaine-binding aptamer in different concentrations of ammonium acetate. No signal was observed for the 5- charge state in pure water. The error bars represent the measurement uncertainty due to the arrival time resolution of the instrument.

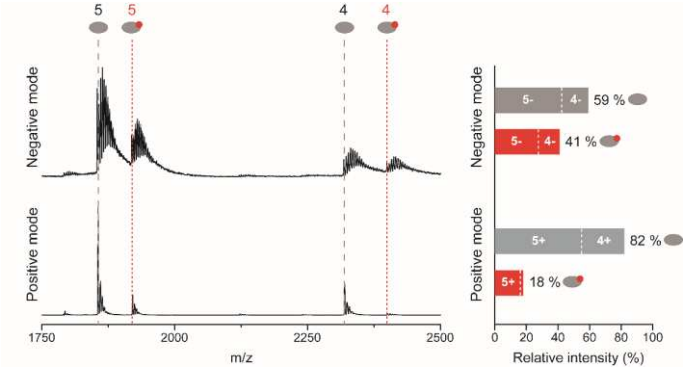

Figure 3. Native IM-MS measurements in the negative and positive ionization mode of the MN19 cocaine-binding aptamer incubated with quinine at a 1:1 molar ratio in 300 mmol/L ammonium acetate. Lines indicate the theoretical peaks of the apo form (grey, dashed) and complex (red, dotted) for the 5-/+ and 4-/+ charge state. Percentages of the aptamer and the complex signals are represented in the bar graph in grey (top) and red (bottom), respectively.

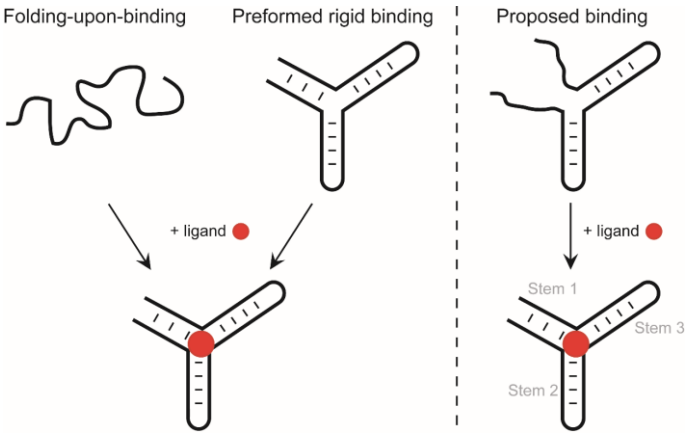

Figure 4. Schematic representation of binding modes for cocaine-binding aptamers with the ligand quinine (red circle). Binding of the ligand might occur via two extreme mechanisms: folding-upon binding of the aptamer and binding to preformed rigid aptamers. Most likely is a scenario in which stem 1 is formed upon binding (proposed binding) as suggested in the literature [53,54].

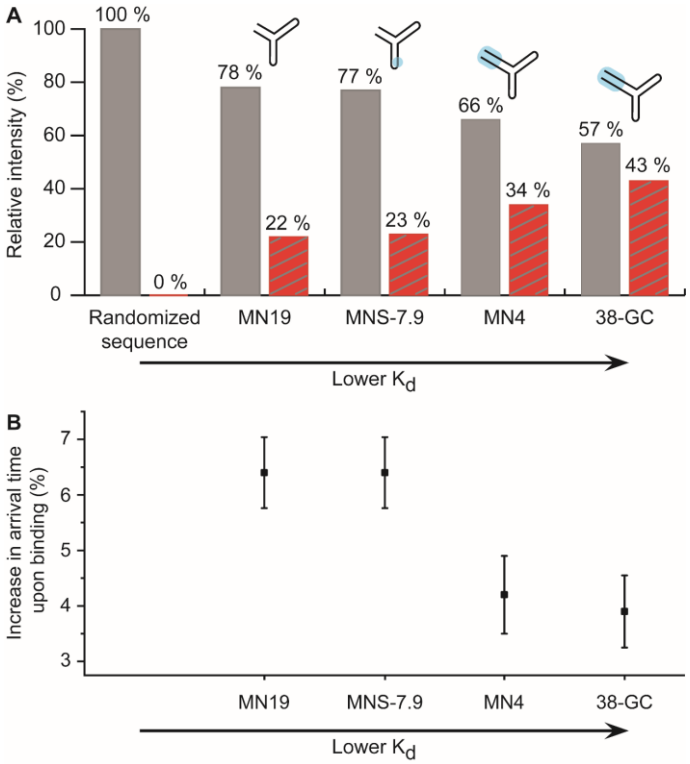

Figure 5. A) Native IM-MS measurements in the positive ionization mode of four cocaine-binding aptamers (MN19, MNS-7.9, MN4, and 38-GC) and a randomized sequence incubated with quinine at a 1:1 molar ratio in 300 mmol/L ammonium acetate. The abundance of the apo form (grey filled area) and complex (red hatched area) are indicated for all aptamers. B) The percentage increase in arrival time upon complexation for the four cocaine-binding aptamers (MN19, MNS-7.9, MN4 and 38-GC).